

Time Averaging Limits and Baseline Dependent Averaging for the ngVLA

ngVLA Computing Memo 8

Jan-Willem Steeb and Zach Gillis

May 3, 2023

Abstract

As of September 2022 a compute capacity of 60 PFLOPS/s is being planned for to flag, calibrate and image ngVLA data [1, p. 73] and [2]. This compute capacity is sufficient to process the majority of ngVLA use cases. However, the spectral line cubes of key science goal 2 require compute in the order of hundreds of PFLOPS/s. In this memo antenna sub-selection with constant time averaging and baseline dependent averaging are evaluated as solutions to reduce the compute requirements. Theoretical calculations and simulations of a single point source at the edge of the science field of view are used to evaluate possible solutions.

By selecting only the antennas necessary to meet the resolution requirements of the spectral line imaging use cases a 30 to 70 times data compression was achieved by using constant time averaging relative to the main array with the same amount of time averaging smearing. However, to meet the sensitivity requirements, observation time has to be increased between 1.8 and 2.4 times. When the entire main sub-array was used baseline dependent averaging provided a 2.5 times reduction in the data volume relative to constant time averaging. However, when the baseline length filtering method was used to select antennas, baseline dependent averaging only provided a 1.7 increase in compression relative to constant time averaging. Consequently, it is not advisable to use baseline dependent averaging by default, since the compression provided is minimal relative to the complexity it introduces to the data processing off-line system for the most strenuous use cases. Nevertheless, for use cases where self calibration is not required it could be advantageous to do baseline dependent averaging before imaging.

1 Introduction

In the literature when the effectiveness of baseline dependent averaging is evaluated it is compared to a high time resolution simulation ([3], [4], [5]) and high compression factors are reported. This memo answers a different question: how effective is baseline dependent averaging compared to constant time averaging with the same signal attenuation. In addition, the effect of removing antennas, so that the synthesized beam's resolution is reduced to that required by the science use case, on constant time averaging and baseline dependent averaging is also explored. The ngVLA science use cases used in this memo are given in table 1 and use cases 2 and 4 will be explored in depth.

When visibility data is baseline dependent averaged shorter baselines can have longer integration times than longer baselines, since the angular speed of the shorter baselines through the uv-plane is slower. Consequently, the visibility data has a more optimal compression relative to constant time averaging. However, it does complicate the visibility data structure, since the number of time steps and integration times for each baseline will be different. This will require other pipeline functions, such as calibration, to do the appropriate interpolation and weighting. In addition, the short baseline integration time may be so long that the variations in environmental effects such as the atmosphere, are no longer well sampled which impacts calibration. Due to these restraints deciding

where averaging occurs is crucial and case dependent. In figure 1 a simplified diagram of the ngVLA off-line data processing pipeline is given along with possible locations for averaging the data. Note that there can be more than one averaging stage. In this memo only the impact of observation geometry on integration time will be explored, however, in the conclusion suggestions will be given of how to integrate the limitations from flagging and calibration.

Simplified ngVLA Data Processing Pipeline

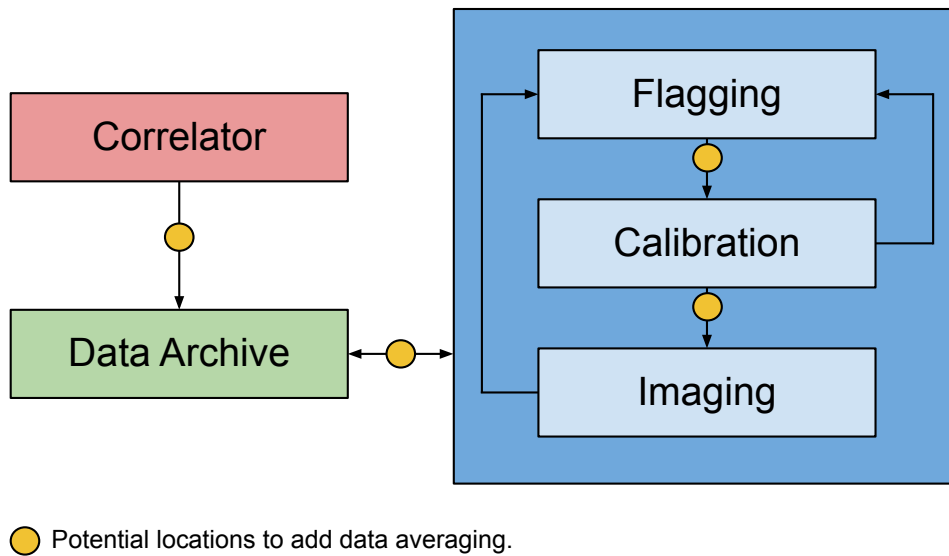


Figure 1

2 Smearing

Since visibility data does not have infinitesimal frequency and time resolution bandwidth smearing and time averaging smearing will occur. Smearing is a decorrelation effect that leads to an attenuation of peak flux and broadening of source structure. Note that the total integrated flux density is preserved.

- **Bandwidth smearing** causes a radial broadening and amplitude attenuation that increases with channel bandwidth and angular distance from the delay tracking center.
- **Time averaging smearing** broadens azimuthally with increasing integration time and is also a function of the elliptical tracks that each baseline makes through the uv-plane longer. When the image is centred on one of the poles the baseline tracks through the uv-plane will be circular and consequently smearing increases with angular distance from the phase tracking center. When the image is not centered at one of the poles a more complicated relationship arises that is a function of image declination and the position of the source (see equation 1).

A diagram of smearing effect is given in figure 2. The main focus of this memo is time averaging smearing.

Use Case	Name	FoV (sci. req.) (arcsec)	FoV (beam) (arcsec)	Res. (sci. req.) (mas)	Center Freq. (GHz)	SA
1	KSG1 Driving Cont Band 6 eg Taurus disk	5.0	35.0	10	100.0	M
2	KSG1 Driving Cont Band 4 eg Taurus disk	5.0	128.4	10	27.3	M
3	KSG2 Driving Line Band 5 eg Sgr B2(N)	60.0	86.5	100	40.5	M
4	KSG2 Driving Line Band 4 eg Sgr B2(N)	60.0	128.4	100	27.3	M
5	KSG2 Driving Line Band 3 eg Sgr B2(N)	60.0	213.7	100	16.4	M
6	KSG3 Driving Line Band 5 eg COSMOS	86.5	86.5	1000	40.5	S + C
7	KSG3 Driving Line Band 4 eg COSMOS	128.4	128.4	1000	27.3	S + C
8	KSG3 Driving Line Band 3 eg COSMOS	213.7	213.7	1000	16.4	S + C
9	KSG3 Driving Line Band 6 eg Spiderweb galaxy	5.0	48.7	100	72.0	M
10	KSG3 Driving Line Band 5 eg Spiderweb galaxy	5.0	97.3	100	36.0	M
11	KSG3 Driving Line Band 4 eg Spiderweb galaxy	5.0	126.5	100	27.7	M
12	KSG3 Driving Line Band 6 eg Virgo Cluster	31.1	31.1	100	112.5	S + C
13	KSG3 Driving Line Band 1 eg M81 Group	2502.9	2502.9	1000	1.4	S + C
14	KSG3 Driving Line Band 1 eg M81 Group	2502.9	2502.9	60000	1.4	C
15	KSG5 Driving Cont Band 1 OTF Find LIGO event	1460.0	1460.0	1000	2.4	M
16	KSG5 Driving Cont Band 4 OTF Find LISA event	128.4	128.4	1000	27.3	S + C
17	KSG5+4 Driving Cont Band 2 OTF Find BHs	443.6	443.6	1000	7.9	S + C
18	KSG5 Driving Cont Band 3 Gw170817@200Mpc	1.0	213.7	1	16.4	LBA
Use Case	Science use case number.					
Name	Key science goal (KSG) code with a short description.					
FoV (sci. req.) (arcsec)	Field of view, in arcseconds, required by the science use case.					
FoV (beam) (arcsec)	Field of view, in arcseconds, determined by the antenna beam, see equation 7.					
Res. (sci. req) (mas)	The required natural resolution in milliarcsecond, see equation 4.					
Center Freq. (GHz)	Center frequency in GHz.					
SA	The sub-array used: M (Main), S (Spiral), C (Core), LBA (Long Baseline Array).					

Table 1: ngVLA Science Use Cases from [1, p. 72-73], [6] and [2, p. 8].

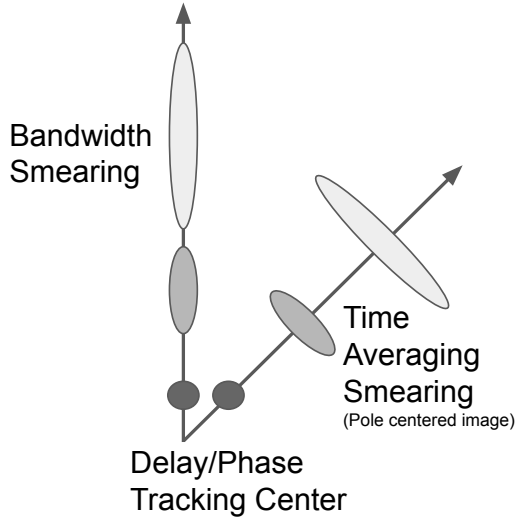


Figure 2: A diagram that shows the effect of radial distance on the distortion (broadening and amplitude attenuation) of a point source caused by bandwidth smearing and time averaging smearing. The darker the shade the higher the intensity.

3 Mathematical Model

Time averaging smearing for an observation cannot be easily expressed mathematically due its dependence on the observation geometry that changes with earth rotation. However, just modelling the source amplitude attenuation component of time averaging smearing is a considerably easier problem. For a visibility integration time τ , a 12-hour observation of a point source with the k^{th} baseline causes a percentage attenuation of the source's amplitude of ([7, p. 380]):

$$\rho_k = 100 \frac{I_{0,k} - I_k}{I_{0,k}} \approx \frac{25\pi^2}{3} \omega_e^2 \tau^2 (l^2 + m^2 \sin^2 \delta) \frac{B_k^2}{\lambda^2}, \quad (1)$$

where

I_k	is the peak response of the source in the image for baseline k ,
$I_{0,k}$	is the peak response in the absence of time averaging smearing,
ω_e	is the angular speed of the Earth's rotation (7.292115910^{-5} rad/s),
τ	is the visibility integration time (s),
δ	is the declination of the phase reference position (rad),
l, m	are the direction cosine coordinates of the source relative to the phase reference position (rad),
$B_k = \Delta X_k^2 + \Delta Y_k^2$	where ΔX_k and ΔY_k are the antenna coordinate differences for the k^{th} baseline in the right handed coordinate system defined in [8, p. 109-110],
λ	is the wavelength corresponding to the center frequency (m).

Equation 1 shows that the percentage amplitude attenuation ρ_k is a function of $(l^2 + m^2 \sin^2 \delta)$ which simplifies to $l^2 + m^2$ when the phase reference position is at one of the poles ($\delta = \pm\pi/2$). By averaging (with equal weight) the percentage amplitude attenuation of all baselines the percentage amplitude attenuation in the naturally weighted image is obtained:

$$\begin{aligned}\rho_{nat} &= \sum_{k=1}^{n_b} \rho_k \approx \frac{25\pi^2\omega_e^2\tau^2(l^2 + m^2 \sin^2 \delta)}{3\lambda^2} \sum_{k=1}^{n_b} \frac{B_k^2}{n_b}, \\ &\approx \frac{25\pi^2\omega_e^2\tau^2(l^2 + m^2 \sin^2 \delta)}{3\lambda^2} \overline{B^2}.\end{aligned}\quad (2)$$

The greatest attenuation (ρ_{min}) will occur when the source is at the edge of the field of view (FoV) so that $l^2 + m^2 \sin^2 \delta = 0.25FoV^2$:

$$\rho_{nat,min} \approx \frac{25\pi^2\omega_e^2\tau^2 FoV^2}{12\lambda^2} \overline{B^2}.\quad (3)$$

Two definitions of field of view (FoV) are referred to in this memo. The first is the beam FoV defined as the full width half maximum (FWHM) of the antenna beam assuming a uniform illumination pattern [9, p. 94]:

$$FoV = \alpha \frac{\lambda}{D}\quad (4)$$

where $\alpha = 1.02$ is the taper coefficient¹ and D is the dish diameter. The second is the science requirement FoV that is determined by the science use case (see table 1).

The maximum integration time for a given percentage amplitude attenuation at the edge of the FoV can now be obtained by solving for τ in equation 3:

$$\tau \approx \sqrt{\frac{3\rho_{nat,min}}{\overline{B^2}} \frac{2\lambda}{5\pi\omega_e FoV}}.\quad (5)$$

Equations 1 to 5 assume a constant integration time, however, shorter baselines have a slower angular speed than longer baselines in the uv-plane, consequently, shorter baselines can have longer integration times than longer baselines. This scheme should lead to a reduction in the data rate relative to constant averaging. One way to implement baseline dependent averaging is to use the UV-distance travelled by a baseline [3, eq. 1]

$$\Delta uvw_{\lambda,max} = \frac{\text{sinc}^{-1}(1 - \frac{\rho_{nat,min}}{100})}{FoV},\quad (6)$$

where $\Delta uvw_{\lambda,max}$ is the maximum distance in the UV plane over which visibility data can be averaged in wavelengths.

4 Antenna Selection

To meet the resolution requirements (see table 1) of the different use cases, not all the baselines in a sub-array are required. The longest necessary baseline (B_{max} in meters) can be calculated using [9, p. 93]:

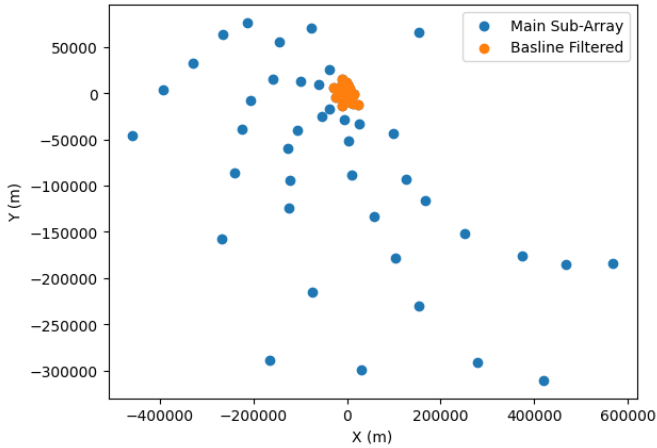
$$B_{max} = k \frac{\lambda}{\theta},\quad (7)$$

¹This number was empirically derived from VLA data.

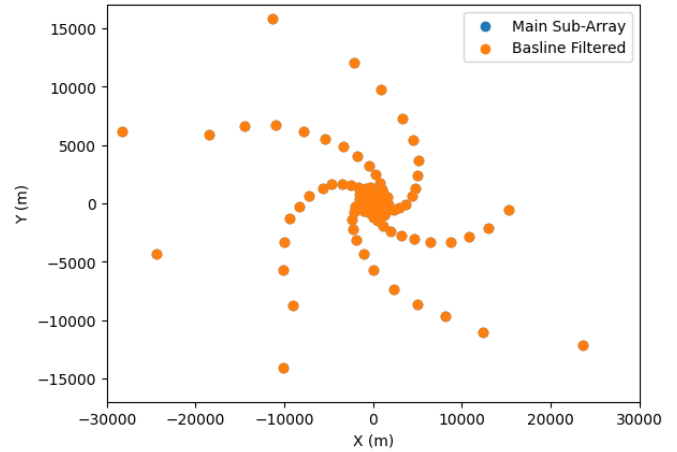
where $k = 0.6$, λ is the wavelength in meters, and θ is the resolution (FWHM) of the naturally weighted synthesized beam. For example, UC4's resolution requirement (10 mas at 27.3 GHz) requires a baseline length of 13.59 km while the longest baseline in the main array is 1036.074 km (for revision D of the array layout [10]). By using shorter baselines the integration time can be increased without leading to significant smearing (see equation 5). The increase in integration time will reduce data rates and compute requirements, however, observation time will have to increase to achieve the sensitivity requirements with fewer antennas.

Two antenna selection strategies are used:

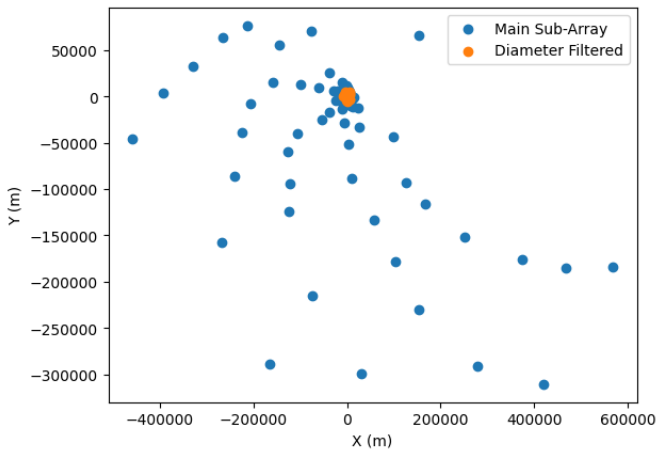
- **Baseline Length Filtering:** All antennas that are part of a baseline with a length less than or equal to the maximum required baseline length, are selected. This antenna selection scheme will lead to longer than required baselines to be included. An example of this is given in figure 3a and 3b.
- **Diameter Filtering:** All antennas that lie within a circle centred at the median antenna position with a diameter equal to the maximum required baseline length, are selected. The diameter of the circle is iteratively increased until a baseline is added that has a length greater than or equal to the maximum required baseline length. An example of this is given in figure 3c and 3d.



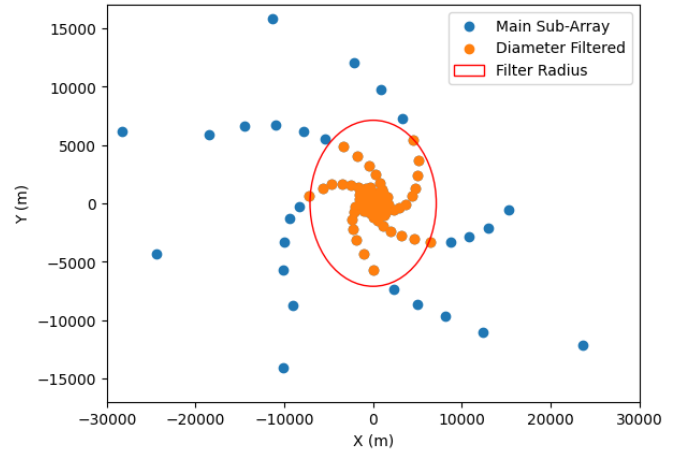
(a) Baseline Length Filtering: Plot of ngVLA main sub-array antenna positions and selected antennas which have baselines with a length less than or equal to the maximum required baseline length.



(b) Baseline Length Filtering: Zoomed in plot of figure a.



(c) Diameter Filtering: Plot of ngVLA main sub-array antenna positions and selected antennas where all antennas lie within a circle such that the resolution requirement is met.



(d) Diameter Filtering: Zoomed in plot of figure c.

Figure 3: Antenna position plots for the ngVLA main array (for revision D of the array layout [10]) where the antennas are selected to meet the resolution requirements for UC4. Figures a and b show the selection done by baseline length filtering and figures c and d show the selection done by diameter filtering.

5 Integration Time and Size of Compute

In this section the results for a 1.0% , 0.5% and 0.1% amplitude attenuation of a source at the edge of the science FoV for each of the use cases in table 1 are presented. Note that only equation 5 was used to calculate the integration times and other constraints such as calibration requirements or observation of transient sources (use case 15-18) were not considered. The use cases whose compute requirements will benefit the most, by reducing the number of long baselines and increasing the integration time, are use case 3-5 that require over an exaFLOPS/s each when the entire main array is used with a 1.0% amplitude attenuation.

Tables 2 and 3 contain the results for the baseline length filtering antenna selection method and tables 4 and 5 contain the results for the diameter filtering antenna selection method. Since the baseline length filtering method will select all antennas that are part of a baseline shorter than or equal to the required baseline length, longer baselines will be included in the filtered sub-array, this can be seen by comparing **B Max. Req** and **B Max Filtered** columns in table 2. For the diameter filtering method the longest baseline length in the filtered sub-array is much closer to the required baseline length (see table 4). The results of these two antenna selection methods show the trade-off that is to be made: by selecting shorter baselines the integration time can be increased which consequently reduces the compute required for processing the data, however selecting shorter baselines leads to fewer antennas in the array which then requires longer observation times to meet the sensitivity requirements.

For example use case 4 requires 0.705 s integration time and 1.287 exaFLOPS/s compute when the entire main array is used with a 1.0% amplitude attenuation. For baseline length filtering the integration time can be increased to 13.08 s and the compute required decreases to 69.38 petaFLOPS/s, however the observation time increases by 1.5 times. The diameter filtering increases the integration time even further to 36.81 s, the compute requirement reduces to 24.65 petaFlops, and the observation time increases by 2.1 times.

Baseline Length Filtering

Use Case (sci. req.) (arcsec)	FoV (beam) (arcsec)	Res. (sci. req.) (mas)	Center Freq. (GHz)	SA	B Max (m)	B Max Req. (m)	B Max Filtered (m)	Antenna Fraction Filtered	1.0% Atten.		0.5% Atten.		0.1% Atten.		Data Comp.	Obs. Time Increase	
									SA	FSA	SA	FSA	SA	FSA			SA
1	5.0	35.0	10	100.0	M	1036074	37102	251208	187/214=0.874	2.310	7.991	1.633	5.650	0.731	2.527	3.459	1.311
2	5.0	128.4	10	27.3	M	1036074	135905	1036074	213/214=0.995	8.461	8.688	5.983	6.144	2.676	2.748	1.027	1.009
3	60.0	86.5	100	40.5	M	1036074	9161	35810	170/214=0.794	0.475	10.650	0.336	7.530	0.150	3.368	22.406	1.587
4	60.0	128.4	100	27.3	M	1036074	13590	54939	173/214=0.808	0.705	13.081	0.499	9.249	0.223	4.136	18.551	1.532
5	60.0	213.7	100	16.4	M	1036074	22623	87432	178/214=0.832	1.174	13.967	0.830	9.877	0.371	4.417	11.900	1.447
6	86.5	86.5	1000	40.5	S+C	35169	916	7817	130/168=0.774	7.975	29.129	5.639	20.597	2.522	9.211	3.652	1.673
7	128.4	128.4	1000	27.3	S+C	35169	1359	11082	139/168=0.827	7.971	21.865	5.636	15.461	2.521	6.914	2.743	1.463
8	213.7	213.7	1000	16.4	S+C	35169	2262	20766	153/168=0.911	7.972	13.177	5.637	9.318	2.521	4.167	1.653	1.206
9	5.0	48.7	100	72.0	M	1036074	5153	35169	168/214=0.785	3.208	77.611	2.269	54.879	1.014	24.543	24.191	1.625
10	5.0	97.3	100	36.0	M	1036074	10306	44063	171/214=0.799	6.416	132.448	4.537	93.655	2.029	41.884	20.642	1.568
11	5.0	126.5	100	27.7	M	1036074	13394	54939	173/214=0.808	8.339	154.701	5.897	109.390	2.637	48.921	18.551	1.532
12	31.1	31.1	100	112.5	S+C	35169	3298	27255	163/168=0.970	7.986	9.448	5.647	6.681	2.525	2.988	1.183	1.062
13	2502.9	2502.9	1000	1.4	S+C	35169	26501	35169	168/168=1.000	7.974	7.974	5.638	5.638	2.522	2.522	1.000	1.000
14	2502.9	2502.9	60000	1.4	C	3454	442	3454	114/114=1.000	43.274	43.274	30.599	30.599	13.684	13.684	1.000	1.000
15	1460.0	1460.0	1000	2.4	M	1036074	15459	54939	174/214=0.813	0.330	5.774	0.233	4.082	0.104	1.826	17.517	1.514
16	128.4	128.4	1000	27.3	S+C	35169	1359	11082	139/168=0.827	7.971	21.865	5.636	15.461	2.521	6.914	2.743	1.463
17	443.6	443.6	1000	7.9	S+C	35169	4696	35169	168/168=1.000	7.973	7.973	5.638	5.638	2.521	2.521	1.000	1.000
18	1.0	213.7	1	16.4	LBA	8845523	2262316	8845523	30/30=1.000	2.609	2.609	1.845	1.845	0.825	0.825	1.000	1.000

Use Case The science use case, see table 1.

FoV (sci. req.) (arcsec) Field of view, in arcseconds, required by the science use case.

FoV (beam) (arcsec) Field of view, in arcseconds, determined by the antenna beam, see equation 7.

Res. (sci. req) (mas) The required natural resolution in milliarcsecond, see equation 4.

Center Freq. (GHz) Center frequency in GHz.

SA The sub-array used: M (Main), S (Spiral), C (Core), LBA (Long Baseline Array).

B Max (m) The longest possible baseline in the sub-array in meters.

B Max Req. (m) The longest baseline required to meet the **Res. (sci. req) (mas)**, see equation 4.

B Max Filtered (m) The longest baseline in the filtered sub-array (**FSA**)

Antenna Fraction Filtered The fraction of antennas in the filtered sub-array **FSA** relative to entire sub-array **SA**.

Int. Time (s) The visibility integration time required so that the amplitude of a point source at the edge of

the **FoV (sci. req.) (arcsec)** does not reduce by more than 1.0%, 0.5%, and 0.1%.

Data Comp. Data compression achieved by using longer integration time of the filtered sub-array (**FSA**)

relative to the sub-array (**SA**) (it is constant for all amplitude attenuation levels).

Obs. Time Increase The factor by which the observation time must be increased, so that the filtered sub-array (**FSA**)

observation has the same sensitivity as the entire sub-array (**SA**) observation.

Table 2: Required visibility integration times for 18 ngVLA science use cases (see [1, p. 72-73]) so that the amplitude attenuation of a point source at the edge of the science field of view (**FoV (sci. req.) (arcsec)**) is equal to 1.0%, 0.5%, and 0.1%. The integration times are calculated using equation 5 and the revision D ngVLA antenna layouts (see [10]). The integration times are also given for the baseline length filtered (see section 4) sub-arrays (**FSA**) that select all antennas in a sub-array (**SA**) that are part of a baseline with a length less than the baseline length required (**B Max. Req (m)**) so that the resolution (**Res. (sci. req) (mas)**) is achieved. This antenna selection scheme will lead to longer than required baselines to be included (the longest baseline in the filtered sub-array is given in **B Max Filtered (m)**). The data compression (**Data Comp.**) achieved by using a filtered sub-array (**FSA**) is only a function of integration time and not the number of antennas used, since the observation time will have to be increased (see **Obs. Time Increase**) to meet the sensitivity requirements. The required size of compute is given in table 3. In table 4 the results for a more restraining sub-array filtering scheme is given, where the **FSA** integration times are longer.

Baseline Length Filtering

Use Case	1.0% Atten.		0.5% Atten.		0.1% Atten.		1.0% Atten.		0.5% Atten.		0.1% Atten.	
	SA	FSA	SA	FSA	SA	FSA	SA	FSA	SA	FSA	SA	FSA
1	0.101	0.029	0.143	0.041	0.320	0.093	0.035	0.010	0.050	0.014	0.111	0.032
2	0.027	0.027	0.039	0.038	0.086	0.084	0.028	0.028	0.040	0.039	0.090	0.087
3	1287.111	57.444	1820.185	81.238	4070.286	181.656	227.322	10.146	321.470	14.348	718.869	32.083
4	1287.137	69.382	1820.217	98.121	4069.776	219.403	227.327	12.254	321.476	17.330	718.780	38.750
5	1279.371	107.507	1809.154	152.037	4045.253	339.966	225.956	18.987	319.523	26.852	714.450	60.043
6	4.721	1.293	6.677	1.828	14.930	4.088	0.834	0.228	1.179	0.323	2.637	0.722
7	4.731	1.724	6.690	2.439	14.959	5.453	0.836	0.305	1.182	0.431	2.642	0.963
8	4.783	2.894	6.764	4.092	15.125	9.150	0.845	0.511	1.195	0.723	2.671	1.616
9	0.022	0.001	0.031	0.001	0.069	0.003	0.004	0.000	0.005	0.000	0.012	0.001
10	0.011	0.001	0.015	0.001	0.035	0.002	0.002	0.000	0.003	0.000	0.006	0.000
11	0.008	0.001	0.012	0.001	0.026	0.001	0.001	0.000	0.002	0.000	0.005	0.000
12	2.546	2.152	3.601	3.044	8.052	6.806	0.450	0.380	0.636	0.537	1.422	1.202
13	1.727	1.727	2.443	2.443	5.462	5.462	0.042	0.042	0.059	0.059	0.132	0.132
14	0.003	0.003	0.004	0.004	0.009	0.009	0.000	0.000	0.000	0.000	0.001	0.001
15	35.667	2.036	50.433	2.880	112.822	6.439	12.385	0.707	17.512	1.000	39.175	2.236
16	0.219	0.080	0.310	0.113	0.693	0.253	0.076	0.028	0.107	0.039	0.240	0.088
17	12.672	12.672	17.920	17.920	40.071	40.071	0.142	0.142	0.200	0.200	0.448	0.448
18	0.010	0.010	0.014	0.014	0.032	0.032	0.004	0.004	0.005	0.005	0.012	0.012
Use Case	The science use case number, see table 1.											
FLOPS/s	Floating point operations per second required, for each use case, when using a sub-array (SA) and filtered sub-array (FSA), defined in table 2.											
GB/s	Data rates (GB/s) required, for each use case, when using a sub-array (SA) and filtered sub-array (FSA), defined in table 2.											

Table 3: The required size of compute using the integration times in table 2.

Diameter Filtering

Use Case (sci. req.) (arcsec)	FoV (beam) (arcsec)	FoV (sci. req.) (mas)	Res. (mas)	Center Freq. (GHz)	SA (m)	B Max (m)	B Max Req. (m)	B Max Filtered (m)	Antenna Fraction Filtered	1.0% Atten.		0.5% Atten.		0.1% Atten.		Data Comp.	Obs. Time Increase
										SA	FSA	SA	FSA	SA	FSA		
1	5.0	35.0	10	100.0	Main	1036074	37102	39890	171/214=0.799	2.310	48.685	1.633	34.426	0.731	15.396	21.077	1.568
2	5.0	128.4	10	27.3	Main	1036074	135905	149052	182/214=0.850	8.461	65.004	5.983	45.965	2.676	20.556	7.683	1.384
3	60.0	86.5	100	40.5	Main	1036074	9161	9369	138/214=0.645	0.475	34.190	0.336	24.176	0.150	10.812	71.934	2.411
4	60.0	128.4	100	27.3	Main	1036074	13590	14221	147/214=0.687	0.705	36.806	0.499	26.026	0.223	11.639	52.199	2.124
5	60.0	213.7	100	16.4	Main	1036074	22623	24007	162/214=0.757	1.174	35.817	0.830	25.326	0.371	11.326	30.516	1.748
6	86.5	86.5	1000	40.5	Spiral + Core	35169	916	924	53/168=0.315	7.975	142.438	5.639	100.719	2.522	45.043	17.860	10.180
7	128.4	128.4	1000	27.3	Spiral + Core	35169	1359	1411	65/168=0.387	7.971	103.438	5.636	73.141	2.521	32.710	12.977	6.744
8	213.7	213.7	1000	16.4	Spiral + Core	35169	2262	2395	91/168=0.542	7.972	61.207	5.637	43.280	2.521	19.355	7.678	3.426
9	5.0	48.7	100	72.0	Main	1036074	5153	5264	125/214=0.584	3.208	344.159	2.269	243.357	1.014	108.832	107.275	2.941
10	5.0	97.3	100	36.0	Main	1036074	10306	10427	140/214=0.654	6.416	428.713	4.537	303.146	2.029	135.571	66.815	2.342
11	5.0	126.5	100	27.7	Main	1036074	13394	14221	147/214=0.687	8.339	435.291	5.897	307.797	2.637	137.651	52.199	2.124
12	31.1	31.1	100	112.5	Spiral + Core	35169	3298	3417	115/168=0.685	7.986	43.071	5.647	30.456	2.525	13.620	5.394	2.140
13	2502.9	2502.9	1000	1.4	Spiral + Core	35169	26501	27255	165/168=0.982	7.974	9.071	5.638	6.414	2.522	2.868	1.138	1.037
14	2502.9	2502.9	60000	1.4	Core	3454	442	464	35/114=0.307	43.274	238.857	30.599	168.897	13.684	75.533	5.520	10.825
15	1460.0	1460.0	1000	2.4	Main	1036074	15459	17368	152/214=0.710	0.330	14.368	0.233	10.159	0.104	4.543	43.591	1.986
16	128.4	128.4	1000	27.3	Spiral + Core	35169	1359	1411	65/168=0.387	7.971	103.438	5.636	73.141	2.521	32.710	12.977	6.744
17	443.6	443.6	1000	7.9	Spiral + Core	35169	4696	4765	124/168=0.738	7.973	36.310	5.638	25.675	2.521	11.482	4.554	1.839
18	1.0	213.7	1	16.4	LBA	8845523	2262316	2296024	12/30=0.400	2.609	7.514	1.845	5.313	0.825	2.376	2.880	6.591

Use Case The science use case, see table 1.

FoV (sci. req.) (arcsec) Field of view, in arcseconds, required by the science use case.

FoV (beam) (arcsec) Field of view, in arcseconds, determined by the antenna beam, see equation 7.

Res. (sci. req) (mas) The required natural resolution in milliarcsecond, see equation 4.

Center Freq. (GHz) Center frequency in GHz.

SA The sub-array used: M (Main), S (Spiral), C (Core), LBA (Long Baseline Array).

B Max (m) The longest possible baseline in the sub-array in meters.

B Max Req. (m) The longest baseline required to meet the **Res. (sci. req)** (mas), see equation 4.

B Max Filtered (m) The longest baseline in the filtered sub-array (FSA)

Antenna Fraction Filtered The fraction of antennas in the filtered sub-array **FSA** relative to entire sub-array **SA**.

Int. Time (s) The visibility integration time required so that the amplitude of a point source at the edge of the **FoV (sci. req.) (arcsec)** does not reduce by more than 1.0%, 0.5%, and 0.1%.

Data Comp. Data compression achieved by using longer integration time of the filtered sub-array (**FSA**) relative to the sub-array (**SA**) (it is constant for all amplitude attenuation levels).

Obs. Time Increase The factor by which the observation time must be increased, so that the filtered sub-array (**FSA**) observation has the same sensitivity as the entire sub-array (**SA**) observation.

Table 4: Required visibility integration times for 18 ngVLA science use cases (see [1, p. 72-73]) so that the amplitude attenuation of a point source at the edge of the science field of view (**FoV (sci. req.) (arcsec)**) is equal to 1.0%, 0.5%, and 0.1%. The integration times are calculated using equation 5 and the revision D ngVLA antenna layouts (see [10]). The integration times are also given for diameter filtered (see section 4) sub-arrays (**FSA**) that select all antennas in a sub-array (**SA**) that lie within a circle centred at the median antenna position with a diameter that is iteratively increased until there is at least one baseline with a length greater than or equal to the baseline required (**B Max. Req (m)**). The data compression (**Data Comp.**) achieved by using a filtered sub-array (**FSA**) is only a function of integration time and not the number of antennas used, since the observation time will have to be increased (see **Obs. Time Increase**) to meet the sensitivity requirements. The required size of compute is given in table 5. In table 2 the results for a less restraining sub-array filtering scheme is given, where the **FSA** integration times are shorter.

Diameter Filtering

Use Case	FLOPS						GB/s					
	1.0% Atten.		0.5% Atten.		0.1% Atten.		1.0% Atten.		0.5% Atten.		0.1% Atten.	
	SA	FSA	SA	FSA	SA	FSA	SA	FSA	SA	FSA	SA	FSA
1	0.101	0.005	0.143	0.007	0.320	0.015	0.035	0.002	0.050	0.002	0.111	0.005
2	0.027	0.004	0.039	0.005	0.086	0.011	0.028	0.004	0.040	0.005	0.090	0.012
3	1287.111	17.893	1820.185	25.305	4070.286	56.583	227.322	3.160	321.470	4.469	718.869	9.993
4	1287.137	24.658	1820.217	34.872	4069.776	77.976	227.327	4.355	321.476	6.159	718.780	13.772
5	1279.371	41.925	1809.154	59.291	4045.253	132.577	225.956	7.404	319.523	10.472	714.450	23.415
6	4.721	0.264	6.677	0.374	14.930	0.836	0.834	0.047	1.179	0.066	2.637	0.148
7	4.731	0.364	6.690	0.515	14.959	1.153	0.836	0.064	1.182	0.091	2.642	0.204
8	4.783	0.623	6.764	0.881	15.125	1.970	0.845	0.110	1.195	0.156	2.671	0.348
9	0.022	0.000	0.031	0.000	0.069	0.001	0.004	0.000	0.005	0.000	0.012	0.000
10	0.011	0.000	0.015	0.000	0.035	0.001	0.002	0.000	0.003	0.000	0.006	0.000
11	0.008	0.000	0.012	0.000	0.026	0.001	0.001	0.000	0.002	0.000	0.005	0.000
12	2.546	0.472	3.601	0.668	8.052	1.493	0.450	0.083	0.636	0.118	1.422	0.264
13	1.727	1.518	2.443	2.147	5.462	4.801	0.042	0.037	0.059	0.052	0.132	0.116
14	0.003	0.001	0.004	0.001	0.009	0.002	0.000	0.000	0.000	0.000	0.001	0.000
15	35.667	0.818	50.433	1.157	112.822	2.587	12.385	0.284	17.512	0.402	39.175	0.898
16	0.219	0.017	0.310	0.024	0.693	0.053	0.076	0.006	0.107	0.008	0.240	0.018
17	12.672	2.782	17.920	3.935	40.071	8.799	0.142	0.031	0.200	0.044	0.448	0.098
18	0.010	0.004	0.014	0.005	0.032	0.011	0.004	0.001	0.005	0.002	0.012	0.004
Use Case	The science use case, see table 1.											
FLOPS/s	Floating point operations per second required, for each use case, when using a sub-array (SA) and filtered sub-array (FSA), defined in table 4.											
GB/s	Data rates (GB/s) required, for each use case, when using a sub-array (SA) and filtered sub-array (FSA), defined in table 4.											

Table 5: The required size of compute using the integration times in table 4.

Use Case	2	4	4
Antenna Selection ¹	All	All	Baseline Filtering ¹
Sub-Array Layout	Main revision D [10]		
Phase Center	J2000 0h00m00.0s 45d00m00.0s		
Frequency	27.3 GHz		
Observation Time (τ_0)	12 hours		
Integration Time	0.4 s	0.02 s	0.4 s
Source Position (l=m)	4.08 rad	24.49 rad	24.49 rad

Table 6: Simulation Parameters.

¹ See section 4 for description of antenna selection methods.

6 Simulation Setup

All simulation work was done using SiRIUS (Simulation of Radio Interferometry from Unique Sources) simulator [11]. Three simulations were done, all the simulations consisted of a single channel and point source such that $l^2 + m^2 \sin^2 \delta = 0.25 F o V^2$ and $l = m$. Table 6 contains the simulation parameters. The integration times of the simulations (τ_0) are chosen so that there is no significant time averaging smearing.

The simulations were first used to verify equation 5, where the derivation includes approximating the sin function with the first term of its Maclaurin series. For each simulation the integration time was varied by averaging the visibilities data. The CASA task `mstransform` was found to be unusably slow in averaging due to not being able to parallel process a single measurement set and the large data sizes of simulated measurement sets (especially the use case 4 simulation that has 1.5 TB of visibility data). Consequently, averaging code was written that is built upon the `SiRIUS software framework` that efficiently runs in parallel.

The percentage amplitude attenuation of the averaged data was calculated using the weighted sum of the absolute value of all the visibilities:

$$\rho_{sim}(\tau) = 100 \left(1 - \frac{\sum_i^{n_{vis}} W_i |V_i|}{I_0 \sum_i^{n_{vis}} W_i} \right) \quad (8)$$

τ is the integration time that the visibilities have been averaged to,

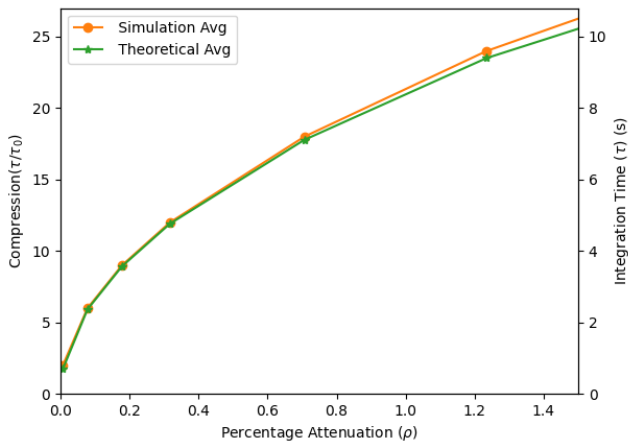
I_0 is the peak response in the absence of time averaging smearing,

V_i is the i^{th} complex visibility value,

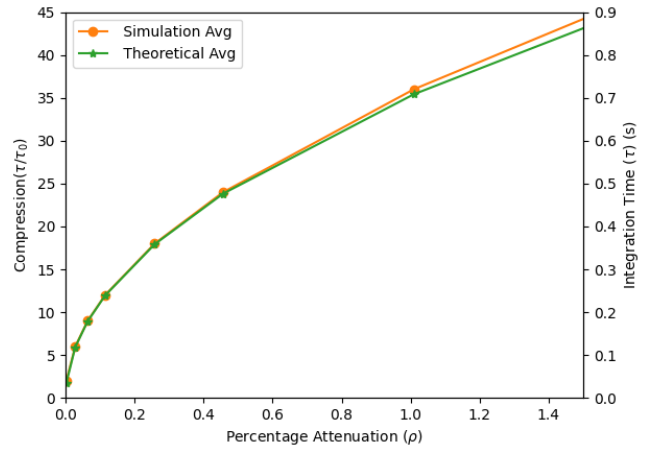
W_i is the weight associated with the i^{th} visibility,

$n_{vis} = (\tau_0/\tau)n_{vis,0}$ is the number of visibilities after averaging.

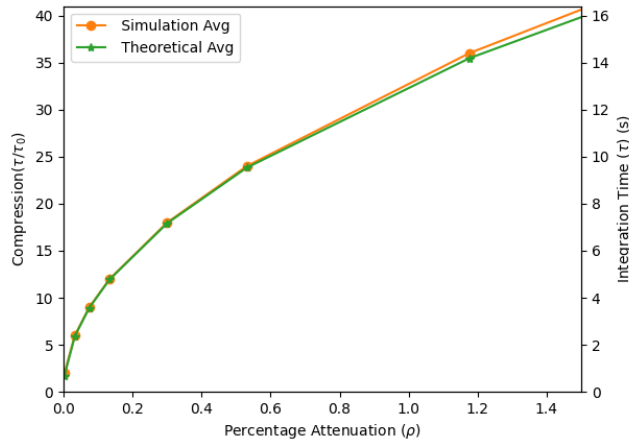
In figures 4 a to c compression (τ/τ_0) is given as a function of the percentage amplitude attenuation (ρ). The theoretical calculation (equation 5) closely follows the simulated results (equation 8) and as expected slowly diverges as the amplitude decreases.



(a) Compression as a function of percentage amplitude attenuation for use case 2 using the entire main sub-array.



(b) Compression as a function of percentage amplitude attenuation for use case 4 using the entire main sub-array.



(c) Compression as a function of percentage amplitude attenuation for use case 4 using the baseline length filtered main sub-array.

Figure 4: Compression as a function of percentage amplitude attenuation for the theoretical calculations (equation 5) and simulations (equation 8).

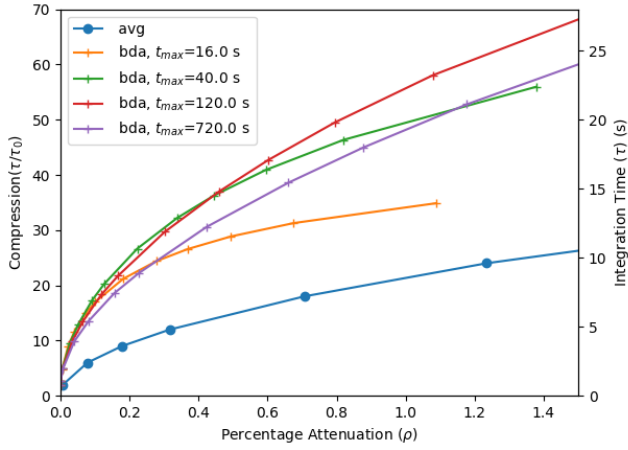
7 Baseline Dependent Averaging

The three simulated datasets (see section 6) were baseline dependent averaged according to equation 6 with software developed using the [SiRIUS software framework](#). The effectiveness of baseline dependent averaging was determined by comparing the compression it achieved with that of constant time averaging for the same attenuation in amplitude. The plots in figure 5 show plots of the compression as function of amplitude attenuation for the three simulations and table 7 shows relative compression values extracted from the graphs for 1.0 %, 0.5 % and 0.1 % attenuation in amplitude. These figures and table also show the effect of varying the maximum allowed integration time for baseline dependent averaging, which is important for cases where self calibration is required.

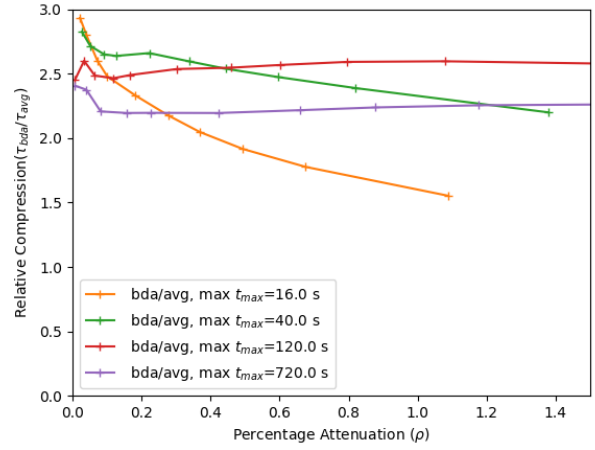
For use cases 2 and 4 the achieved relative compression is similar (see figures 5b and 5d), since constant time averaging and baseline dependent averaging both can be increased by a decrease in the FoV (see equations 5 and 6) and the only difference between the simulations for use cases 2 and 4 is that the FoV for the use case 2 simulation is smaller. For the baseline length filtered use case 4 simulation the relative compression achieved using baseline dependent averaging is lower than that achieved by the two other simulations, because the filtered array no longer has the long baselines (see figure 3).

Use Case 2				
Max Integration Time (s)	Relative Compression			
	1.0 % Atten.	0.5 % Atten.	0.1 % Atten.	
16.0	1.6	1.9	2.5	
40.0	2.3	2.5	2.7	
120.0	2.6	2.6	2.4	
720.0	2.2	2.2	2.1	
Use Case 4				
Max Integration Time (s)	Relative Compression			
	1.0 % Atten.	0.5 % Atten.	0.1 % Atten.	
2.0	1.9	2.2	2.6	
8.0	2.6	2.6	2.5	
36.0	2.3	2.3	2.1	
Use Case 4 Baseline Length Filtered				
Max Integration Time (s)	Relative Compression			
	1.0 % Atten.	0.5 % Atten.	0.1 % Atten.	
16.0	1.2	1.4	1.7	
40.0	1.7	1.7	1.6	
60.0	1.7	1.7	1.6	
720.0	1.6	1.6	1.6	

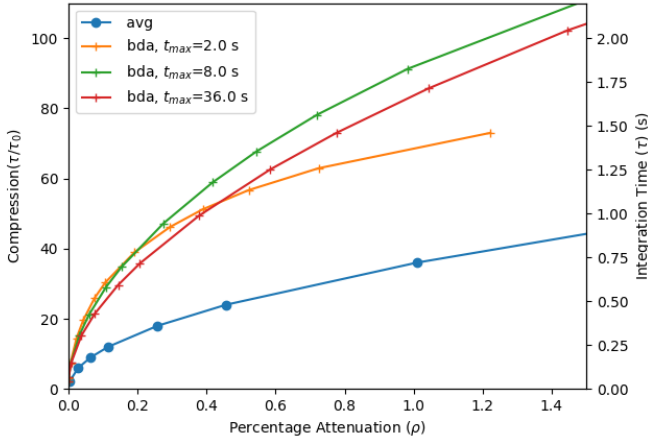
Table 7: Table of the compression that baseline dependent averaging achieves over that of constant time averaging for the same amplitude attenuation for each of the ngVLA simulations (see section 6).



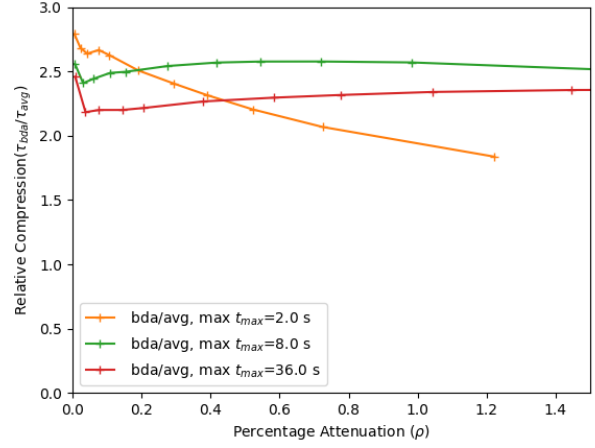
(a) Use case 2.



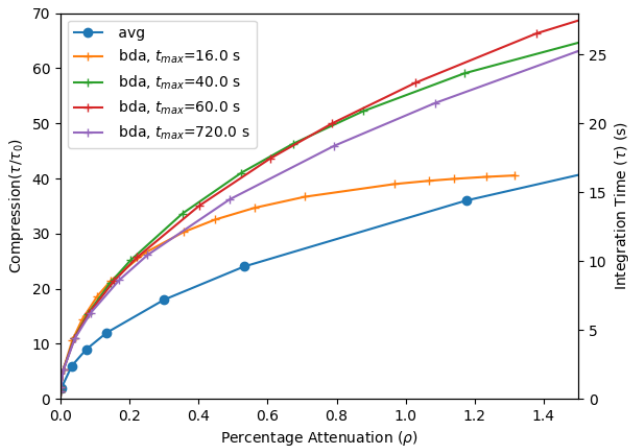
(b) Use case 2.



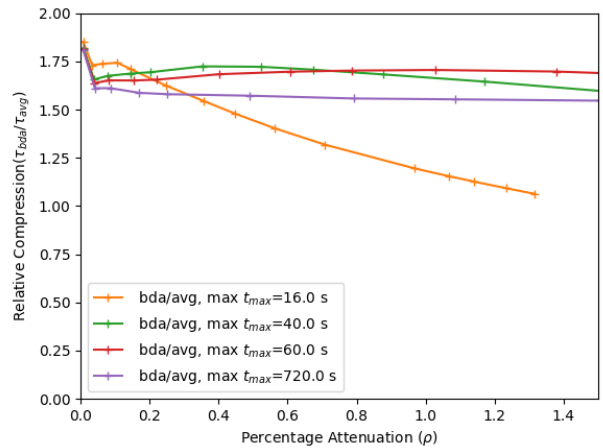
(c) Use case 4.



(d) Use case 4.



(e) Use case 4 with baseline length filtering.



(f) Use case 4 with baseline length filtering.

Figure 5: The plots show for each of the ngVLA simulations (see section 6) how constant time averaging (avg in legend) and baseline dependent averaging (bda in legend) can compress the data for a given percentage amplitude attenuation. In plots a,c and d the compression is relative to the original simulation and plots b,d,f give the compression that baseline dependent averaging achieves over that of constant time averaging. For baseline dependent averaging the maximum integration time is also varied (t_{max} in legend).

8 Conclusion

Only selecting the antennas required to meet the science use case resolution requirements had the greatest impact on reducing the compute requirements of the most compute intensive ngVLA use cases 4,5,6 (KSG2). For example, using the diameter filtering method to select antennas and constant time averaging for use case 4 reduced the compute requirements by a factor of 52 times. However, it requires a 2.1 times longer observation to meet the sensitivity requirements.

Baseline dependent averaging provided a further 2.5 times reduction in the data volume relative to constant time averaging when the entire main sub-array was used for use case 4. However, when the baseline length filtering method was used to select antennas, baseline dependent averaging only provided a 1.7 increase in compression when compared to constant time averaging. Consequently, it is not advisable to use baseline dependent averaging, since the compression provided is minimal relative to the complexity it introduces to the data processing off-line system for the most strenuous use cases. Nevertheless, for use cases where self calibration is not required it could be advantageous to do baseline dependent averaging before imaging.

The following recommendation will make use of three maximum integration times: τ_{flag} is the maximum integration time allowed such that RFI can be correctly detected and flagged, τ_{cal} is the maximum allowed integration time so that environmental and instrumental effects are correctly sampled, and τ_{img} is the maximum integration time allowed due to the geometry of the observation so that time averaging smearing is at an acceptable level:

- **Self calibration required:** Integration time of data going into data archive is given by $\min(\tau_{flag}, \tau_{cal}, \tau_{img})$.
- **No self calibration required:** Integration time of data going into data archive is given by $\min(\tau_{flag}, \tau_{cal}, \tau_{img})$. Before calibration if $\tau_{cal} > \tau_{flag}$ and $\tau_{cal} < \tau_{img}$ the data should be averaged to τ_{cal} . Before imaging if $\tau_{img} > \tau_{cal}$ and $\tau_{img} > \tau_{flag}$ then the data should be averaged to τ_{img} . Furthermore, any averaging should only be done if it results in a significant reduction in data.

References

- [1] R. Selina et al., “System Conceptual Design Description,” *National Radio Astronomy Observatory*, August 2022, <https://ngvla.nrao.edu/download/MediaFile/364/original>.
- [2] S. Bhatnagar et al., “Size-of-Computing Estimates for ngVLA Synthesis Imaging ngVLA Computing Memo #4,” *National Radio Astronomy Observatory*, August 2021, https://library.nrao.edu/public/memos/ngvla/NGVLAC_04.pdf.
- [3] W. Cotton, “Effects of baseline dependent time averaging of uv data,” National Radio Astronomy Observatory, Jun. 8, 2009, <http://www.cv.nrao.edu/~bcotton/ObitDoc/BLAverage.pdf>.
- [4] S. J. Wijnholds et al., “Baseline-dependent averaging in radio interferometry,” *Monthly Notices of the Royal Astronomical Society*, May 2018, <https://doi.org/10.1093/mnras/sty360>.
- [5] M. Atemkeng et al., “Xova: Baseline-Dependent Time and Channel Averaging for Radio Interferometry,” ADASS2020: Astronomical Data Analysis Software and Systems XXX, 27 Jan 2021, <https://arxiv.org/abs/2101.11270>.
- [6] J. M. Wrobel et al., “A Notional Reference Observing Program,” *National Radio Astronomy Observatory*, January 2020, <https://ngvla.nrao.edu/download/MediaFile/249/original>.

- [7] A. H. Bridle and F. R. Schwab, “Synthesis Imaging in Radio Astronomy II: Bandwidth and Time-Average Smearing,” *Astronomical Society of the Pacific Conference Series*, vol. 180, Jan. 1999, pp. 371–381, <https://adsabs.harvard.edu/full/1999ASPC..180..371B>.
- [8] A. R. Thompson et al., “Interferometry and Synthesis in Radio Astronomy,” Third Edition, 2017, Springer Open, <https://link.springer.com/content/pdf/10.1007/978-3-319-44431-4.pdf>.
- [9] R. Selina et al., “ngVLA System Requirements,” *National Radio Astronomy Observatory*, May 2020, <https://ngvla.nrao.edu/download/MediaFile/254/original>.
- [10] ngVLA Team, “ngVLA Tools & Materials: Configuration Revision D,” *National Radio Astronomy Observatory*, August 2022, <https://ngvla.nrao.edu/page/tools>.
- [11] J. Steeb et al., “SiRIUS: Simulation of Radio Interferometry from Unique Sources,” *National Radio Astronomy Observatory*, <https://sirius-sim.readthedocs.io/en/latest/about.html>.